EPJ manuscript No.
(will be inserted by the editor)

Memory effect and anisotropy of particle arrangements in granular paste

So Kitsunezaki[1a], Arina Sasaki[1], Akihiro Nishimoto[2], Tsuyoshi Mizuguchi[3], Yousuke Matsuo[4], and Akio Nakahara[4]

[1] Research Group of Physics, Division of Natural Sciences, Faculty of Nara Women's University - Nara 630-8506,Japan
[2] Faculty of Health and Well-being, Kansai University, Sakai 590-8515, Japan
[3] Department of Mathematical Sciences, Osaka Prefecture University, Sakai 599-8531, Japan
[4] Laboratory of Physics, College of Science and Technology, Nihon University, Funabashi 274-8501, Japan

Received: date / Revised version: date

Abstract. It is known that pastes of fine powder, for example those of clay, retain memory of shaking applied early in a drying process. This memory results in the appearance of anisotropic patterns of desiccation cracks after drying. In this work, we find a similar behavior in pastes consisting of large granular particles, specifically cornstarch and Lycopodium spores. Because of the large particle size, we were able to observe particle arrangements in Lycopodium paste with micro-focus X-ray computerized tomography (μCT). We prepared pastes consisting of Lycopodium particles and water. Agar was added to the paste in order to allow for solidification during a drying process. In these samples, we found statistical anisotropy induced by shaking applied early in the drying process. This anisotropy possesses a feature that was predicted on the basis of results obtained in previous experimental and theoretical studies.

PACS. 46.50.+a Fracture mechanics, fatigue and cracks – 46.35.+z Viscoelasticity, plasticity, viscoplasticity – 83.80.Hj Suspensions, dispersions, pastes, slurries, colloids

1 Introduction

Mixtures of fine granular particles and liquid behave as an elasto-plastic fluid when the solid volume fraction is in an intermediate range. The lower and upper boundaries of this range are referred to as the "liquid" and "plastic" limits, respectively. Such paste-like mixtures have the ability to remember the direction of an external perturbation. The existence of this memory has been confirmed by the observation of anisotropic patterns of desiccation cracks formed when the mixtures are dried [1,2]. In such experiments, several types of memory effects have been observed in systems prepared using various types of clay, solid volume fractions, and types of external perturbations [3–7]. The formation of anisotropic crack patterns induced by external fields has also been studied for the purpose of application to the control of crack formation [8,9].

The *memory of shaking* is the most thoroughly investigated memory effect of drying paste. When a layer of paste is dried after horizontal shaking applied for a short time, parallel cracks first appear in the direction perpendicular to the initial shaking under the effect of memory of shaking, and then short cracks form in the parallel direction to release stresses induced in resultant long rectangular fragments, resulting in a ladder-type pattern. It has been found that such a memory effect exists only when paste is subjected to shear stresses larger than the yield stress during the initial shaking. This type of memory effect has been found for pastes of clay and pastes consisting of major constituents of clay, such as kaolin, calcium carbonate ($CaCO_3$) and magnesium carbonate hydroxide, and for mixtures of activated charcoal powder and water [1–4]. It has been found that, in such pastes using smaller solid volume fractions or adding sodium chloride can result in another type of memory effect, referred to as *memory of flow*. In this case, if flow is created in paste initially, for example, by strong shaking or gravity, cracks appear first in the direction parallel to the initial flow direction after drying [3,5].

We have not yet determined what structures in paste are responsible for the memory effects described above. It has been found that anisotropic crack patterns resulting from the memory of shaking form even if the upper region of the paste layer is removed before crack formation. This leads us to conclude that this memory is retained near the bottom of the paste layer, not in the wrinkles or microcracks appearing on the upper surface [1]. Elasto-plastic theories have been proposed to understand the memory effect of shaking. Using such theories, it has been hypothesized that the memory effect results from anisotropy in residual stresses caused by initial shaking [7,10–12]. In a previous study, we estimated horizontal stresses in $CaCO_3$ paste by measuring the bending displacements of plate

[a] *e-mail:* kitsune@ki-rin.phys.nara-wu.ac.jp

springs attached to the bottom of the container. We confirmed that the tension parallel to the initial shaking is slightly larger than the tension in the perpendicular direction, and we identified this anisotropy as the memory of shaking. The difference between the tensions in these two directions is approximately 1/10 of these values, and we found that this difference increases with the tensions until drying causes the first crack formation [13].

In this study, we succeeded in observing microscopic structures responsible for the memory effect of shaking. We carried out drying experiments on systems consisting of two types of paste composed of larger granules, cornstarch particles and Lycopodium spores. We confirmed that both types of pastes exhibit the memory of shaking, as described in Sec. 2. We next investigated the memory effect of shaking in Lycopodium paste using μCT. We found anisotropic structures of the arrangement of particles depending on the direction of the shaking. Our method and results are reported in Sec. 3.

2 The memory effect in granular paste

Both cornstarch and Lycopodium particles have roughly round shapes and are more uniform in size than powders commonly used in drying experiments, such as heavy calcium carbonate. As thermal Brownian motion is negligible for such large particles, mixtures of them and water form pastes of granular materials (granular pastes) that cannot be regarded as colloidal material [14]. We performed drying experiments on systems consisting of both types of paste and confirmed that the memory effect of shaking appears in both. Our results are described in the following two subsections. The morphological diagrams of desiccation crack patterns for these systems have features in common with the diagram for $CaCO_3$ paste [1]. These results suggest that the memory effect of shaking appears in the same manner for many types of paste and that it is insensitive to the surface properties of the powder under investigation.

2.1 Cornstarch paste

Cornstarch particles have diameters of approximately 15 μm and are essentially insoluble in water at room temperature. The mass density of a particle is $1.55 - 1.60\mathrm{g/cm^3}$, which changes slightly through the absorption of water. In this paper, we ignore the absorption of water and adopt the mass density $1.59\mathrm{g/cm^3}$, measured by Brown et al [15], to calculate the solid volume fraction ϕ from the cornstarch-to-water mixing ratio.

Because the precipitation of starch particles occurs readily, due to the difference in density between starch particles and water, ordinary drying experiments cannot yield reproducible results for suspensions of cornstarch. For this reason, we applied vertical vibrations to stir the paste just prior to the horizontal shaking. For this purpose, our system was placed on a vertical vibration machine, L-0505 (Asahi Seisakusyo, Tokyo, Japan), and this

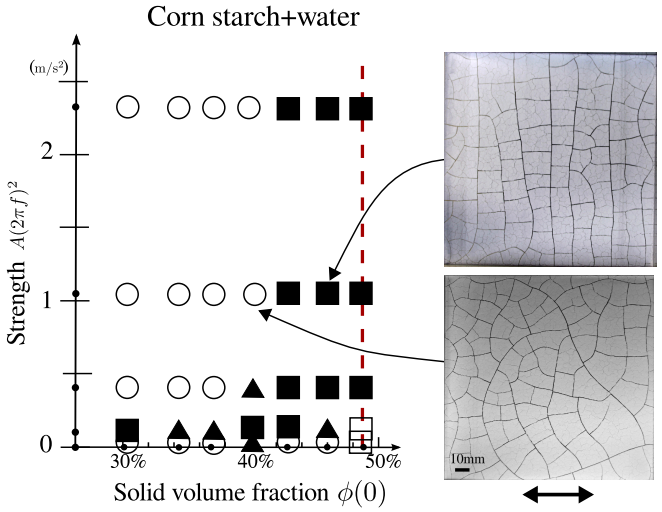

Fig. 1. Morphological phase diagram of desiccation cracks in cornstarch paste. Horizontal shaking was applied at the beginning of the drying pastes in the direction indicated by the arrow just after vertical vibrations. The unshaded circles and the shaded squares indicate situations in which isotropic crack patterns and lines of cracks perpendicular to the horizontal shaking appeared, respectively. The shaded triangles indicate the appearance of incomplete or partial anisotropic patterns. In the region indicated by the unshaded squares, crack patterns due to the vertical vibrations [6] were observed even after the horizontal shaking was applied. The dashed line indicates the plastic limit of $\phi(0) = 48.7\%$ measured by Brown et al. [15]

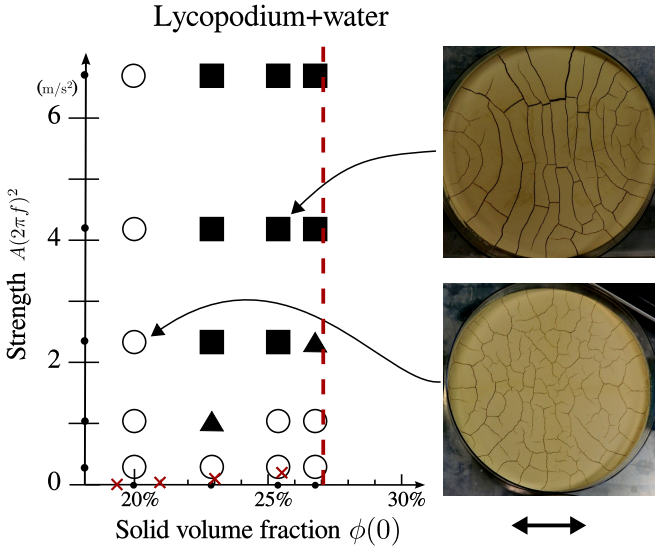

Fig. 2. Morphological phase diagram of desiccation cracks in Lycopodium paste. Horizontal shaking was applied in the direction indicated by the arrow. The paste was defoamed by stirring in vacuum before the experiments, and here, no vertical vibration was applied. The definitions of the symbols are the same as in Fig. 1. The weight of a sample was 9.77 ± 0.14g when it was dried completely. The values of the yield stress, σ_Y, divided by the mass of the paste per unit area are plotted by the "x" symbols, and the dashed line indicates the plastic limit.

configuration rested on a horizontal shaker, FNX-220 (TGK, Tokyo, Japan). The paste system was contained in an acrylic container with a square, horizontal bottom ($146 \times 146\text{mm}^2$) that was fixed to the vibration machine.

In an experiment, we poured a mixture of 50.0g of cornstarch powder (*Wako* Pure Chemical Industries, Osaka, Japan) and ion-exchanged water into the acrylic container. We then subjected the system to vertical vibrations with a frequency in the range $65 - 80$Hz and an amplitude in the range $0.5 - 1.5$mm for approximately 1min. The frequency and amplitude were chosen such that the vibrations would generate Faraday waves in order to stir the mixture thoroughly. Immediately after the vertical vibrations were applied, we applied horizontal shaking with a frequency $f(= 8, 25, 50, 80, 120\text{rpm})$ and an amplitude $A = 15$mm for approximately 1min, and then left the sample undisturbed to dry at room temperature. The layer thickness of the paste was $3 - 5$mm before drying.

Figure 1 displays a morphological diagram of the resulting crack patterns. The horizontal and vertical axes represent the initial solid volume fraction, $\phi(0)$, and the maximum acceleration of the horizontal shaking, $A(2\pi f)^2$, respectively. The maximum acceleration determines the maximum shear stress exerted on paste by shaking. These quantities were varied by controlling the water fraction of the paste and the shaking frequency, f. We confirmed that only isotropic crack patterns are formed when no horizontal shaking is applied, although the effect of the vertical oscillation[6] was observed at a large solid volume fraction near the plastic limit.

In the region indicated by the shaded squares, lines of cracks perpendicular to the direction of the horizontal shaking were formed. It was difficult to thoroughly stir mixtures of cornstarch and water to make a uniform paste for values of $\phi(0)$ larger than the right boundary of this region. The right boundary approximately corresponds to the plastic limit measured by Brown et al., $\phi(0) = 48.7\%$[15]. In addition, we found that a layer of supernatent resulting from sedimentation vanishes as $\phi(0)$ approaches the right boundary. It is inferred that the yield stress for compression due to their own weight also increases as $\phi(0)$ approaches the plastic limit [16–18]. On the left-hand side of this region, the memory effect seems to exist even for very small solid volume fractions if the frequency is sufficiently small. We believe that the reason for this is that the solid volume fraction increases significantly near the bottom due to sedimentation during slow horizontal shaking.

2.2 Lycopodium paste

Spores of *Lycopodium clavatum* take the form of rounded tetrahedra with a finely meshed surface. They are approximately 30μm in diameter. Their surfaces are hydrophobic, because their main constituent is fatty oil. For this reason, it was necessary to stir the mixture of these spores and water for a long time to make a uniform paste. Here, precipitation does not have an important effect, as the density of a Lycopodium spore is 1.05g/cm^3, close to that of water.

We prepared a mixture of Lycopodium powder (Association of Powder Process Industry and Engineering, Japan) and ion-exchanged water and stirred it in vacuum to remove small bubbles. Pouring the paste into a circular polystyrene Petri dish with diameter 141.6mm, we applied horizontal shaking of frequency $f(= 40, 80, 120, 160, 200\text{rpm})$ and amplitude $A = 15$mm using a shaker FNX-220 for 5min. We then allowed the paste to dry at room temperature. No vertical vibration was applied in advance. The total weight of the paste was chosen such that the weight of the Lycopodium powder was 10g. The corresponding initial layer thickness depended on $\phi(0)$, and it was approximately $2 - 3$mm.

Figure 2 displays a morphological diagram for Lycopodium paste. In the region indicated by the shaded squares, lines of cracks perpendicular to the direction of shaking appeared. Results at larger values of $\phi(0) > 26.6\%$ were not be obtained, because horizontal shaking could not spread paste throughout the container in such situations. The left and right boundaries of this region correspond to the liquid and the plastic limits, respectively, as in the diagram for $CaCO_3$ paste. We measured shear rates in a coaxial double cylindrical vessel using a rheometer, Physica MCR301 (Anton Paar, Austria), and estimated the yield stresses σ_Y from the onset of rotational motion in the case that the applied torque increased. We measured $\sigma_Y = 0.036 \pm 0.009$, 0.077 ± 0.016, 0.23 ± 0.04 and 0.48 ± 0.07Pa for $\phi(0) = 19.4, 21.0, 23.0$ and 25.5%, respectively. It thus seem that σ_Y effectively vanishes at the left boundary. Contrastingly, σ_Y increases drastically as the right boundary is approached, with $\sigma_Y = 150 \pm 60$Pa for $\phi(0) = 27.0\%$. We found that Lycopodium paste exhibits discontinuous shear thickening, like cornstarch paste [15, 19].

3 μCT observations of particle arrangements

We examined whether there exists anisotropy in the arrangement of Lycopodium particles in paste. As the best resolution of μCT scanning is a few μm, Lycopodium pastes are the most appropriate for the observation of the arrangement of particles because of their large particle size. We took three-dimensional images using a μCT device, SMX-225CT (*Shimadzu*, Kyoto, Japan) at the laboratory of *Shimadzu* Techno-Research Inc. in Kyoto, Japan. A sample was rotated slowly on a turntable in the device during each scanning. After approximately 1/2 hour of scanning, we obtained a 3-d image composed of equally spaced cross-sections of a cylindrical region in the paste for each sample.

3.1 Experimental method

We added cesium chloride (CsCl, *Wako* Pure Chemical Industries, Osaka, Japan) to the ion-exchanged water in an amount equal to 14% of water content, by weight. This was

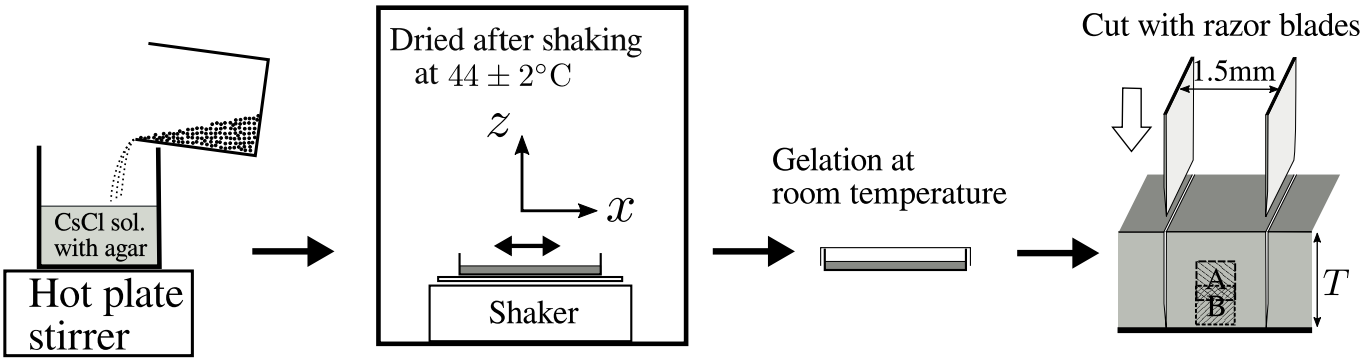

Sample	Solid volume fraction before drying → at gelation time	Order of cutting (top view)	Scanning region (Diameter × Height)	N	z
Agar1	22.7% → 30.0%(after all cracking had finished)	= → ‖	A: 905μmϕ × 813μm	14901	6.36
Agar2	23.4% → 28.7%(at the first cracking)	= → ‖	B: 907μmϕ × 815μm	18225	6.60
Agar3	22.9% → 26.6%(just before cracking)	= → ‖	B: 898μmϕ × 810μm	13814	5.05
Agar4	22.8% → 27.9%(at the first cracking)	‖ → =	B: 934μmϕ × 803μm	18279	6.22

Fig. 3. Preparation of a sample and the scanning conditions. The centers of the cylindrical scanning regions A and B were located at a position of approximately 1/2 and 1/4 of the layer thickness from the bottom, respectively. A pixel in the 3-d X-ray image obtained corresponds to a cube with sides of length $D/1024$ in the paste, where D is the diameter of the cylindrical scanning region. Agar1-3 were cut in the direction parallel to the initial shaking and then in the perpendicular direction. The order of cutting was reversed for Agar4, to confirm that the cutting protocol did not affect the arrangement of particles. N and z represent the number and the average coordination number of the detected particles, respectively. The detection efficiency was estimated to vary within 10% depending on the image quality. In the case of Agar1, the value of N was smaller than it would be expected from the value of ϕ alone, because in this case, there was a significant amount of air bubbles, which existed mainly in the upper region of the paste.

necessary because the particles could not be observed in pure water, due to small difference in the X-ray absorption coefficient for water and the particles. The concentration of the CsCl solution was 0.80M, and the mass density was 1.10g/cm^3. This mass density is slightly larger than that of a Lycopodium particle. We confirmed that the morphological diagram of the crack patterns was not significantly altered by the addition of CsCl (diagram omitted).

In the μCT measurements, because the region outside of the scanned region introduces noise into the image, it was necessary to make the samples sufficiently small that their images were not affected by this noise. In order to prepare small samples, we solidified paste layers during the drying process by the introduction of agar into paste.

As depicted in Fig. 3, we dissolved a small amount of agar (used for tissue culturing, *Ina* Food Industry, Japan) into a hot CsCl solution and then mixed Lycopodium powder to make a sample of paste. This agar solution gelates at temperatures below approximately 40°C. The initial proportion of agar was 0.4g per 100g of water. Unlike in the case described by Fig. 2, in the present case, we did not defoam the paste in vacuum, in order to avoid desiccation and a decrease of temperature.

We poured paste into a circular polystyrene Petri dish of diameter 141.6mm. This was then placed on a shaker WKN-2240 (*Waken* B Tech., Kyoto, Japan) in a high temperature environment of 44 ± 2°C to avoid gelation of the agar. We next allowed the sample to dry after applying a horizontal oscillation of amplitude $A = 12.5$mm and frequency $f = 60$rpm for approximately 5min.

After the drying process progressed up to the point at which the solid volume fraction was such that cracks appeared, we placed a lid on the sample to prevent further desiccation, and allowed it to solidify at room temperature. The paste subsequently solidified softly. The crack pattern remained unchanged during this gelation process, except for the slight elongation of previously existing cracks. The sample was covered until the μCT observation, carried out approximately one day after gelation. We report the scanning results for the four samples of Lycopodium paste, Agar1-4. Their details are listed in the table appearing in Fig. 3. Every sample contained 10g of Lycopodium powder, and $\phi(0)$ was approximately 23%. In the drying process, $20 - 35$% of the water in the paste was lost, and thus ϕ and the density of the agar increased accordingly. The layer thickness was initially approximately 3.0 mm, and decreased to $T \simeq 2.2 - 2.5$ mm until gelation.

Just prior to the μCT observations, we cut the layer of paste vertically with a pair of parallel razor blades (produced for microtomes by Kenis, Osaka, Japan) along the directions parallel and perpendicular to the initial horizontal shaking. In this way, we obtained a block of paste of size $1.5 \times 1.5 \times T$mm^3. This block was attached gently to the top of a long plastic rod with double-faced adhesive tape and capped to prevent desiccation. This rod was then fixed vertically on the turntable for scanning.

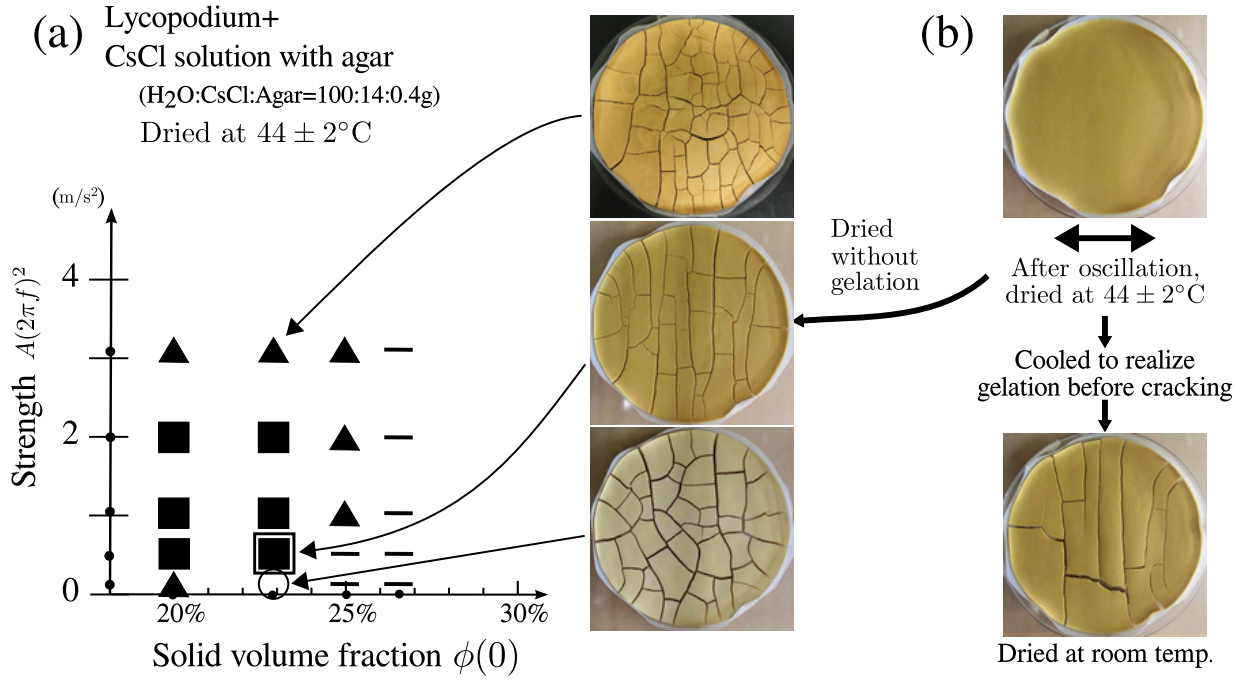

Fig. 4. (a) Morphological diagram of crack patterns for a paste consisting of Lycopodium powder and a CsCl solution with agar. The values of $\phi(0)$ were calculated from the mass densities of the powder and the CsCl solution by assuming that the small amount of agar is negligible. The samples were prepared and dried in the high temperature environment, as explained in Sec. 3.1 The minus signs indicate the region in which the paste did not spread throughout the container evenly during shaking, due to large yield stresses. (b) An anisotropic crack pattern also appeared in a sample that solidified before crack formation and then dried at room temperature.

We found that the addition of agar causes slight changes in the region in which the memory effect appears in the morphological diagram as shown in Fig. 4(a). From this result, we speculate that increasing the viscosity of the solution affects the rheological properties of the paste. The shaded square enclosed by a larger square indicates the conditions used for the four samples investigated here.

We found that the memory of shaking is not lost through the gelation process caused by the agar. In order to confirm this, we removed a sample of paste from the high temperature environment before crack formation and dried the solidified sample at room temperature until cracking. As shown in Fig. 4(b), in this case also, cracks perpendicular to the direction of shaking appeared, although the crack spacing was slightly larger than in the case in which the sample remained in the high temperature environment until after crack formation. Also, when the sample was removed from the high temperature environment before cracking, peeling of the paste at the bottom of the sample was often observed.

3.2 Results

Figures 5 (a) and (b) display typical cross sections of the μCT images. These cross sections correspond to a horizontal plane in each sample. A block of paste was fixed in scanning in such a manner that the x axis of the μCT images approximately corresponded to the direction of the shaking, although the method we used to orient these samples had a typical error in the range $10 - 20°$.

The arrangement of particles seems to be rather random in these images. However, they exhibit a statistical anisotropy. In order to analyze a 3-d image, we first determined the center of mass coordinates $\boldsymbol{r}_i (i = 1, 2, \cdots, N)$ for all detected particles after smoothing and binarization by using ImageJ [20], and then we calculated the distribution of the separation vectors $\boldsymbol{r}_{ij} \equiv \boldsymbol{r}_i - \boldsymbol{r}_j$. Figure 6 displays the distributions of neighboring particles in the horizontal plane for the four samples investigated here. The 3-d polar coordinates (r, α, β) were used to express $\boldsymbol{r}_{ij}$. The maximum peaks located near $r = 30\mu$m correspond to the size of a Lycopodium particle, and α is the angle from the direction of the shaking. We find that the density of neighboring particles is large in the direction perpendicular to the shaking ($\alpha \simeq 90, 270°$) for all samples.

In order to quantify the observed anisotropy, we calculated the orientational order parameters

$$S_{kl} \equiv \langle n_k n_l - \frac{1}{3}\delta_{kl} \rangle \quad (k, l = x, y, z), \tag{1}$$

where n_k is the kth component of the unit vector, $\boldsymbol{n} \equiv \boldsymbol{r}_{ij}/|\boldsymbol{r}_{ij}|$, for neighboring particles. Here $\langle \cdots \rangle$ denotes the average over particle pairs in a region satisfying $|\boldsymbol{r}_{ij}| \leq 35\mu$m. The number of detected particles, N, and the average coordination number calculated from the number of

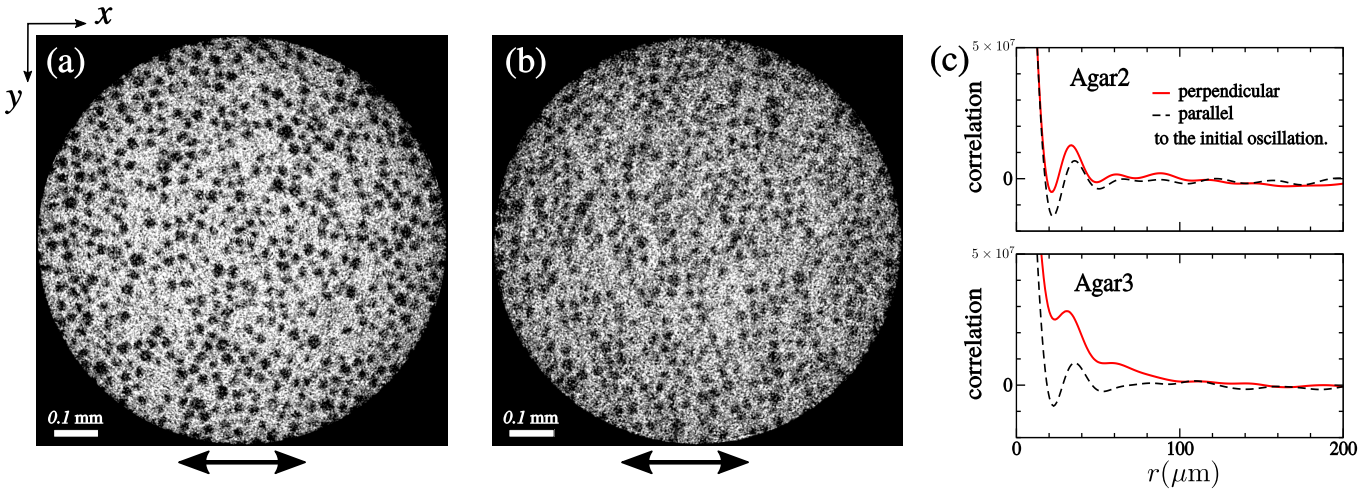

Fig. 5. Typical cross sections of the 3-d μCT raw images (16-bit gray scale) for (a) Agar2 and (b) Agar3. Lycopodium particles appear darker than the surrounding CsCl solution, due to their small X-ray adsorption coefficient. The direction of the shaking was approximately parallel to the x-axis, as indicated by the arrows. Faint concentric circles are artifacts generated as a result of the image construction. (c) Autocorrelation functions (ACF) of μCT images for Agar 2 and Agar 3 in the two directions determined from the orientational order parameters. The red solid curve (black dashed curve) represents the ACF measured along the direction of the projection of $\boldsymbol{u}_1$ ($\boldsymbol{u}_3$) as described in the text. This direction is approximately perpendicular (parallel) to that of the initial shaking.

particle pairs, z, are listed in the table of Fig. 3. We computed the eigenvalues λ_i ($\lambda_1 \geq \lambda_2 \geq \lambda_3$) and the eigenvectors $\boldsymbol{u}_i$ of this matrix. If the distribution of particles is isotropic, all components of this matrix vanish and then $\lambda_1 = \lambda_2 = \lambda_3 = 0$, whereas, if all particles are aligned in one direction, $\lambda_1 = \frac{2}{3}$ and $\lambda_2 = \lambda_3 = -\frac{1}{3}$.

We confirmed that all samples have significant anisotropy. We calculated the square of the matrix norm, $\mathrm{Tr}(S^2) = \sum_{k,l} S_{kl}^2 = \lambda_1^2 + \lambda_2^2 + \lambda_3^2$, for each sample, and checked if it is sufficiently large compared with the statistical error due to finiteness of the number of particles as follows. In the calculation of S_{kl} for each sample, we used a set of $Nz/2$ unit vectors, $\{\boldsymbol{n}\}$, obtained from pairs of neighboring particles. If $\{\boldsymbol{n}\}$ were generated from the isotropic distribution, S would fluctuate around zero, and the magnitude of such fluctuation would be indicated by $\langle \mathrm{Tr}(S^2) \rangle = \frac{4}{3Nz}$. We calculated the values of $q \equiv \frac{3Nz}{4}\mathrm{Tr}(S^2)$ for Agar1-4 and obtained $q = 2.56$, 5.68, 11.1 and 7.32, respectively. The probability that $\frac{3Nz}{4}\mathrm{Tr}(S^2) \geq q$ for the isotropic distribution is 2.5% for $q = 2.56$ and 0.0034% for $q = 5.68$, and then sufficiently small for all samples.

All samples have anisotropy in the same direction in the horizontal plane. As λ_2 was found to be approximately zero for all samples, the maximum eigenvalue, $\lambda_1 \simeq -\lambda_3$, represents the magnitude of the anisotropy, and $\boldsymbol{u}_1$ ($\boldsymbol{u}_3$) corresponds to the direction in which neighboring particles gather most (least). We use circles of radius λ_1 in the plane spanned by $\boldsymbol{u}_1$ and $\boldsymbol{u}_3$ to visualize the results. Figure 7(a) displays the projection of these circles on to the xy plane for the four samples. The fact that the projected circles have circular shapes here indicates that, in this case, the anisotropy exists in the horizontal plane. Fore each circle, the line segment representing the diameter of that circle indicates the direction of $\boldsymbol{u}_1$ in that case. The directions of $\boldsymbol{u}_1$ for the 4 samples are the same within orientational errors of fixation in scanning.

We noted that Agar3 has the largest anisotropy. The main difference between Agar3 and the others is the timing of gelation, as shown in the table of Fig. 3. As Agar3 was solidified before the plastic limit, this result may suggest that the magnitude of anisotropy created by the initial shaking varies in the dry and gelation processes. However we must investigate more samples to clearly identify the reason for this large anisotropy.

Figure 5(c) displays the autocorrelation functions of the μCT images in the directions of $\boldsymbol{u}_1$ and $\boldsymbol{u}_3$ projected on to the horizontal plane, respectively, for Agar2 and Agar3 samples. Because these two directions are inferred to correspond to the directions perpendicular and parallel to the initial shaking, the difference between these two functions represents the anisotropy. The first peaks correspond to neighboring particles. The anisotropy decays over the distance of a few particle diameters for all samples.

In summary, we found the short-range statistical anisotropy that the number of neighboring particles increases in the direction perpendicular to the direction of shaking in the horizontal plane in samples. This is the first observation of anisotropic particle arrangements caused by shaking in paste, and indicates that the memory of shaking is a statistical property of the bulk of the paste, not retained in discontinuous structures, such as small cracks or shear bands.

The microscopic anisotropy found in this study is consistent with the sign of the stress anisotropy found in the previous studies although the effect of shear deformation

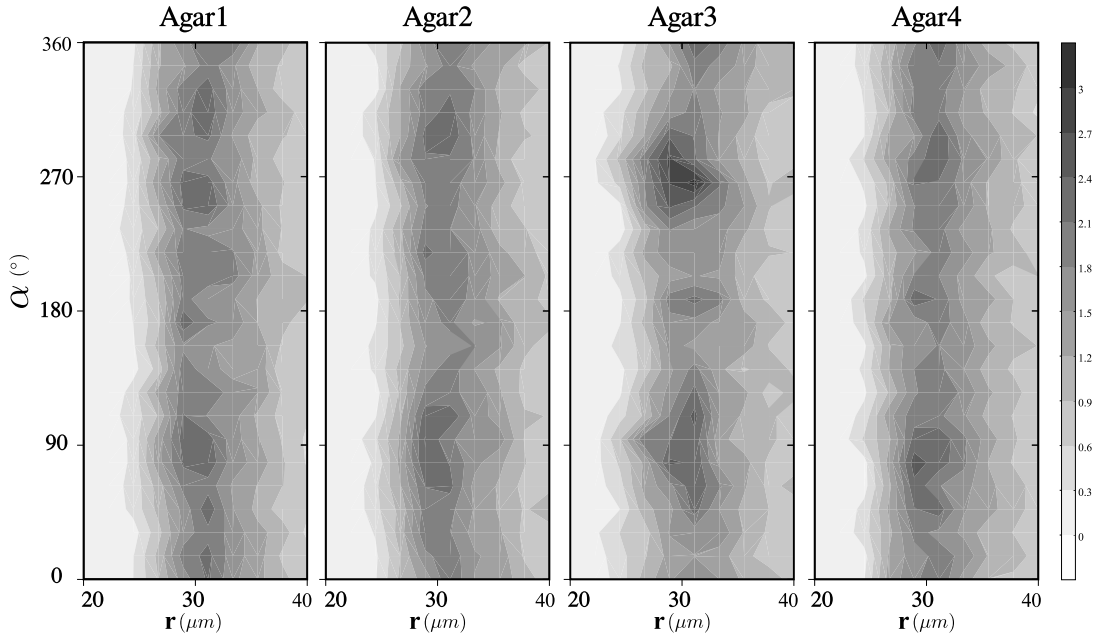

Fig. 6. Distribution of separation vectors to neighboring particles. The coordinates (r, α, β) represent the distance between two particles, $|r_{ij}|$, the angle of $\boldsymbol{r}_{ij}$ projected on to the xy plane from the x axis, and the angle of $\boldsymbol{r}_{ij}$ from the z axis, respectively. The average distributions in the range $80 < \beta \leq 90^\circ$ are plotted with respect to (r, α). Because $\boldsymbol{r}_{ij}$ and $\boldsymbol{r}_{ji}$ contribute equally to the distribution function, we only calculated either vector by filtering $z_{ij} > 0$.

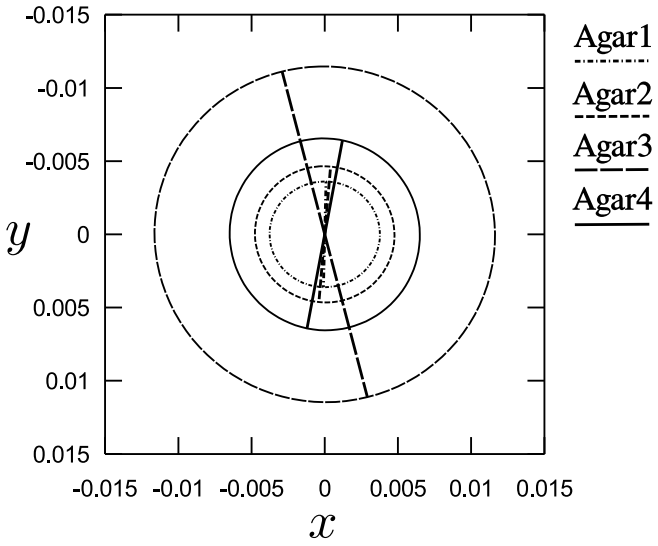

Fig. 7. Circles representing the orientational order parameters for the four samples. The circles are drawn in the plane in which anisotropy appears and projected on to the shear plane. For each circle, the diameter represents the value of the maximum eigenvalue, λ_1, and the direction of the line segment with this length indicates the direction of the corresponding eigenvector, $\boldsymbol{u}_1$. The sum of the eigenvalues is zero, and the second eigenvalue is approximately zero for all samples: $\lambda_1 + \lambda_2 + \lambda_3 = 0$ and $\lambda_2 = -0.0006 \pm 0.0014$.

on granular paste with a yield stress has not been clarified well theoretically. The possible scenario is as follows: Dry shrinkage and corresponding macroscopic tensions are caused by a decrease in the hydrostatic pressures in paste during the drying process [7,21–29]. The pressure difference between fluids in paste and surrounding atmosphere causes isotropic compression to constituent particles, and the response of the particles alters the total stresses to be anisotropic. In the cases in which the main interactions among particles are repulsive, as in the case of elastic contacts, a network of pairs of contacting particles bears dry shrinkage through their repulsive interactions and reduces the tensions caused by the shrinkage. As our μCT observation indicates that the number of such pairs increases in the direction perpendicular to the initial shaking, we expect that tensions decrease more in the perpendicular direction. In previous measurements carried out for $CaCO_3$ paste [13], we found that tensions are the largest in the direction parallel to the shaking, and the sign of the difference between the stresses in parallel and perpendicular directions is consistent with that predicted by residual tension theories [7,10–12].

4 Conclusions

In this study, we experimentally observed the memory effect of shaking in two types of granular paste, cornstarch paste and Lycopodium paste. We also carried out μCT measurements for the Lycopodium paste, through which we found a statistical anisotropy of particle arrangements in paste solidified during the middle stage of the drying

process due to the presence of agar. This anisotropy depends on the direction of the initial shaking in such a manner that the number of neighboring particles increases in the direction perpendicular to the shaking. This is consistent with previous theoretical and experimental results on the memory effect of shaking. The particle arrangements that we observed seem to be rather random, but have significant anisotropy. It is interesting that such weak anisotropy controls the direction of crack growth. The statistical anisotropy can also yield anisotropy of some macroscopic properties, for example, the elastic modulus and the fracture toughness. It is a future project to investigate which anisotropy dominates the growth direction of desiccation cracks.

We have not confirmed how anisotropic structures are created. We are planning to investigate this point by observing the initial anisotropy created before drying and checking whether it changes during a drying process. The method used in this study could also be used to clarify other types of memory effects if we are able to find appropriate pastes consisting of large granular particles.

We acknowledge N. Tsumaki and T. Ojima of *Shimadzu* Techno-Research Inc., and K. Akasaka of *Shimadzu* Science West Corp for the operations and the arrangements of the μCT device. We also thank K. Ishii of Radiation Physics Group of Nara Women's University for his technical advices on μCT, and OOSHIDA T. and M. Otsuki for fruitful discussions on experimental method and data analyses. This research was supported by Grants-in-Aid for Scientific Research (KAKENHI C 26400395 and KAKENHI C 16K05485) from JSPS, Japan.

5 Author contribution statement

All authors contributed substantially to obtaining the results reported in this paper and to the preparation of the manuscript. The memory effect of cornstarch paste was investigated by A. Sasaki as her graduation thesis. The analysis of the separation vectors in the μCT images was carried out mainly by A. Nishimoto.

References

1. A. Nakahara, Y. Matsuo, J. Phys. Soc. Jpn. **74**, 1362 (2005)
2. A. Nakahara, Y. Matsuo, J. Stat. Mech.: Theory Exp., P07016 (2006)
3. A. Nakahara, Y. Matsuo, Phys. Rev. E **74**, 045102(R) (2006)
4. A. Nakahara, Y. Shinohara, Y. Matsuo, J. Phys. : Conf. Ser. **319**, 012014 (2011)
5. Y. Matsuo, A. Nakahara, J. Phys. Soc. Jpn. **81**, 024801 (2012)
6. H. Nakayama, Y. Matsuo, OOSHIDA T., A. Nakahara, Eur. Phys. J. E **36**, 1 (2013)
7. L. Goehring, A. Nakahara, T. Dutta, S. Kitsunezaki, S. Tarafdar, *Desiccation Cracks and their Patterns: Formation and Modelling in Science and Nature*, Statistical Physics of Fracture and Breakdown (Wiley, 2015)
8. L. Pauchard, F. Elias, P. Boltenhagen, A. Cebers, J.C. Bacri, Phys. Rev. E **77**, 021402 (2008)
9. T. Khatun, M.D. Choudhury, T. Dutta, S. Tarafdar, Phys. Rev. E **86**, 016114 (2012)
10. M. Otsuki, Phys. Rev. E **72**, 046115 (2005)
11. OOSHIDA T., Phys. Rev. E **77**, 061501 (2008)
12. OOSHIDA T., J. Phys. Soc. Jpn. **78**, 104801 (2009)
13. S. Kitsunezaki, A. Nakahara, Y. Matsuo, Europhys. Lett. **114**, 64002 (2016)
14. P. Coussot, *Rheometry of Pastes, Suspensions, and Granular Materials* (John Wiley & Sons, Hoboken, New Jersey, 2005)
15. E. Brown, H.M. Jaeger, Phys. Rev. Lett. **103**, 086001 (2009)
16. W.H. Shih, W.Y. Shih, S.I. Kim, I.A. Aksay, J. Amer. Ceram. Soc. **77**, 540 (1994)
17. K.T. Miller, R.M. Melant, C.F. Zukoski, J. Amer. Ceram. Soc. **79**, 2545 (1996)
18. M.D. Green, D.V. Boger, Ind. Eng. Chem. Res. **36**, 4984 (1997)
19. E. Brown, H.M. Jaeger, J. Rheol. **56**, 875 (2012)
20. We used Fiji which is a public domain image processing program based on ImageJ (https://fiji.sc/) and its 3D Object Counter plugin.
21. A.F. Routh, W.B. Russel, Langmuir **15**, 7762 (1999)
22. M.S. Tirumkudulu, W.B. Russel, Langmuir **21**, 4938 (2005)
23. K.B. Singh, M.S. Tirumkudulu, Phys. Rev. Lett. **98**, 218302 (2007)
24. W.B. Russel, N. Wu, W. Man, Langmuir **24**, 1721 (2008)
25. W. Man, W.B. Russel, Phys. Rev. Lett. **100**, 198302 (2008)
26. S. Kitsunezaki, Adv. Powder Technol. **22**, 311 (2011)
27. L. Goehring, W.J. Clegg, A.F. Routh, Phys. Rev. Lett. **110**, 024301 (2013)
28. S. Kitsunezaki, Phys. Rev. E **87**, 052805 (2013)
29. L. Goehring, J. Li, P.C. Kiatkirakajorn, Phil. Trans. R. Soc. A **375**, 20160161 (2017)